

Relaxation dynamics and long-time tails explain shear-induced diffusion of soft athermal particles near jamming

Kuniyasu Saitoh¹ and Takeshi Kawasaki²

¹*Department of Physics, Faculty of Science, Kyoto Sangyo University, Kyoto 603-8555, Japan*

²*Department of Physics, Nagoya University, Nagoya 464-8602, Japan*

(Dated: April 15, 2022)

We numerically study shear-induced diffusion of soft athermal particles in two dimensions. The Green-Kubo (GK) relation is applicable to diffusion coefficient of the particles near jamming, where both mean squared particle velocities and relaxation time included in the GK formula are well explained by critical scaling. We show that auto-correlation functions of the transverse velocities are stretched exponential if the system is below jamming or shear rate is large enough. However, if the system is above jamming and the shear rate is sufficiently small, the auto-correlations exhibit long-time tails such that time integral in the GK formula diverges in two dimensions. We propose empirical scaling relations for the critical exponents and demonstrate that the long-time tails cause finite size effects on the shear-induced diffusion coefficient.

Soft athermal particles, e.g. foam, emulsions, colloidal suspensions, and granular materials, are ubiquitous, and a better understanding of their transport properties is of central importance to technology, e.g. manufacturing processes of food, pharmaceutical and personal care products [1]. It has been well recognized that soft athermal particles exhibit *jamming transition* at a critical packing fraction ϕ_J [2–4], where their mechanical [4, 5] and rheological properties [6–11] can be understood in the context of critical phenomena. For instance, flow curves are nicely explained by critical scaling, i.e. both the viscosity divergence [12–16] and scaling of the yield stress [6, 7] are described as power-laws of the proximity to jamming, $\Delta\phi \equiv \phi - \phi_J$, where ϕ is a packing fraction of the particles.

In contrast, *shear-induced diffusion*, which is relevant to mixing and segregation of soft athermal particles [17], has been studied with the focus on its dependence on a strain rate. Using natural length and time scales, i.e. the particle diameter d_0 and inverse of shear rate $\dot{\gamma}^{-1}$, one can expect a scaling of diffusion coefficient as $D \sim d_0^2 \dot{\gamma}$ [18–22]. However, increasing the shear rate, one observes a crossover from the linear scaling to sub-linear scaling, i.e. from $D \propto \dot{\gamma}$ to $\dot{\gamma}^{0.8}$ [23–26]. Another sub-linear scaling $D \propto \dot{\gamma}^{0.78}$ was also found at the onset of jamming transition, $\phi \simeq \phi_J$ [27]. Moreover, Kharel and Rogon clarified the influence of collective motions of the particles on the shear-induced diffusion and modified the scaling as $D \sim d_0^2 \dot{\gamma} / \sqrt{I}$ with the inertia number I [28–30].

Recently, we demonstrated scaling collapses of the diffusion coefficient near jamming [31], predicting not only the crossover but also the critical divergence of D (that is consistent with the inverse proportionality, i.e. $D \propto p^{-1}$ with the pressure p [21]). It was shown that the diffusion coefficient scales as $D \sim d_0 \xi \dot{\gamma}$ with a characteristic size of collective motions, ξ [28, 32]. If the system is above jamming ($\phi > \phi_J$) and sheared at a sufficiently small strain rate, the size of collective motions extends to the system length, i.e. $\xi \sim L$, such that the diffusion coefficient over

the shear rate linearly scales as $D/\dot{\gamma} \propto L$ [31]. This agrees with numerical results of sheared amorphous solids [33–36] though the finite-size effect was explained as a result of spatially correlated flip events. Note that (slightly) different finite-size scaling, $D/\dot{\gamma} \propto L^{1.05}$ [37, 38] and $L^{1.5}$ [39], was also reported by elastoplastic mesoscale models.

Though the previous studies have revealed relations between diffusion coefficient and length scale, transport properties of thermal systems such as classical fluids and glasses are understood by relaxation dynamics [40–42], and little is known about the role of relaxation time in the shear-induced diffusion of soft athermal particles.

In this Letter, we investigate the shear-induced diffusion by molecular dynamics (MD) simulations. Employing the Green-Kubo (GK) relation for the diffusivity of non-equilibrium soft athermal particles, we clarify the link between diffusion coefficient D and relaxation time extracted from velocity auto-correlation functions. We show that (i) mean squared particle velocities obey critical scaling near jamming, (ii) the relaxation time is also explained by critical scaling only if the system is not in a quasi-static regime above jamming, and (iii) *long-time tails* are observed in the quasi-static regime above jamming such that D formulated by the GK relation diverges in the thermodynamic limit, $L \rightarrow \infty$. We use the reduced GK formula to find (iv) empirical scaling relations of the critical exponents. Our analysis is based on the time scale, where finite-size effects on D are explained by the long-time tails. This is in sharp contrast to the previous studies, where D is connected to the length scale [28–31] and finite-size effects are interpreted as the system spanning flip events [33–39].

Numerical methods.— We perform MD simulations of soft athermal particles in two dimensions. Our system consists of an equal number of small and large particles with diameters, d_0 and $1.4d_0$, respectively [4]. The total number of particles is $N = 8192$ (we examine finite-size effects in later) and their packing fraction ϕ is controlled around the jamming transition density, $\phi_J \simeq 0.8433$ [6].

Repulsive force between the particles, i and j , in contact is modeled as elastic force, $\mathbf{f}_{ij}^e = k\delta_{ij}\mathbf{n}_{ij}$, where k is the stiffness and $\mathbf{n}_{ij} \equiv \mathbf{r}_{ij}/|\mathbf{r}_{ij}|$ with the relative position $\mathbf{r}_{ij} \equiv \mathbf{r}_i - \mathbf{r}_j$ is the normal unit vector. The elastic force is linear in the overlap $\delta_{ij} \equiv R_i + R_j - |\mathbf{r}_{ij}| > 0$, where R_i (R_j) is the radius of the particle i (j). We also add damping force to every particle as $\mathbf{f}_i^d = -\zeta\{\mathbf{v}_i - \mathbf{u}(\mathbf{r}_i)\}$, where ζ , \mathbf{v}_i , and $\mathbf{u}(\mathbf{r})$ are the damping coefficient, particle velocity, and external flow field, respectively. Note that the stiffness and damping coefficient determine a microscopic time scale as $t_0 \equiv \zeta/k$. To simulate simple shear flows, we impose the external flow field in the x -direction as $\mathbf{u}(\mathbf{r}) = (\dot{\gamma}y, 0)$ under the Lees-Edwards boundary condition [43], where $\dot{\gamma}$ is the shear rate. In our simulations, motions of the particles are described by *overdamped dynamics* [6, 7, 44], i.e. $\sum_{j \neq i} \mathbf{f}_{ij}^e + \mathbf{f}_i^d = \mathbf{0}$, where we numerically integrate the particle velocity $\mathbf{v}_i = \mathbf{u}(\mathbf{r}_i) + \zeta^{-1} \sum_{j \neq i} \mathbf{f}_{ij}^e$ with a small time increment $\Delta t = 0.1t_0$.

In the following, we only analyze the data in a steady state, where the shear strain applied to the system exceeds unity, and scale every time and length by t_0 and d_0 , respectively. In addition, we vary ϕ and $\dot{\gamma}$ in the ranges, $0.8 \leq \phi \leq 0.9$ and $10^{-7} \leq \dot{\gamma}t_0 \leq 10^{-2}$, respectively.

Diffusion coefficient and the Green-Kubo relation.— We quantify mass transport of the particles under shear by the transverse component of mean squared displacement (MSD),

$$\Delta(\tau)^2 = \left\langle \frac{1}{N} \sum_{i=1}^N \Delta y_i(t+\tau)^2 \right\rangle_t. \quad (1)$$

Here, $\Delta y_i(t+\tau) \equiv y_i(t+\tau) - y_i(t)$ is the y -component of particle displacement for the duration τ and we take the ensemble average $\langle \dots \rangle_t$ by changing the initial time t in a steady state [31]. The MSD is linear in τ if the amount of shear strain (for the duration τ) exceeds unity, i.e. $\gamma \equiv \dot{\gamma}\tau > 1$. Therefore, a diffusion coefficient can be defined as $D = \lim_{\tau \rightarrow \infty} \Delta(\tau)^2/2\tau$.

In Ref. [31], we demonstrated scaling collapses of the diffusion coefficient near jamming and numerically confirmed its critical scaling as $D \sim |\Delta\phi|^{-\nu}\dot{\gamma}$ ($\phi < \phi_J$), $D \sim |\Delta\phi|^{0.3\lambda-\nu}\dot{\gamma}^{0.7}$ ($\phi > \phi_J$), and $D \sim \dot{\gamma}^{1-\nu/\lambda}$ ($\Delta\phi$ -independent *critical regime*), where the critical exponents are given by $\nu = 1.0$ and $\lambda = 4.0$.

On the other hand, the diffusion coefficient is given by the GK formula [27, 40],

$$D = \langle v_y^2 \rangle \int_0^\infty C(\tau) d\tau. \quad (2)$$

Here, $\langle v_y^2 \rangle \equiv \langle N^{-1} \sum_{i=1}^N v_{iy}(t)^2 \rangle_t$ is the y -component of mean squared particle velocity, where $\langle \dots \rangle_t$ is the time average in a steady state. On the right-hand-side of Eq. (2), $C(\tau) = \langle v_y(t+\tau)v_y(t) \rangle_t / \langle v_y^2 \rangle$ is the normalized velocity auto-correlation function.

Critical scaling of the mean squared velocity.— As the diffusion coefficient D exhibits the critical behavior near jamming [27, 31], the mean squared transverse velocity $\langle v_y^2 \rangle$ in the GK formula (Eq. (2)) can also be explained by critical scaling. Figure 1(a) displays scaling collapses of $\langle v_y^2 \rangle$, where the packing fraction ϕ increases as listed in the legend. In this figure, scaling exponents are given by $\chi = 3.5$ and $\psi = 4.5$, and the solid line with the slope ψ/χ represents the $\Delta\phi$ -independent critical regime. See Supplemental Material (SM) [45] for the x -component of mean squared velocity fluctuation, i.e. $\langle \delta v_x^2 \rangle$ with $\delta v_x \equiv v_x - \dot{\gamma}y$, which shows quantitatively the same critical behavior.

In our numerical model, the energy injected by shear $\dot{\gamma}\sigma$ is dissipated by the damping force \mathbf{f}_i^d , where σ is the shear stress of the system. The rate of energy dissipation can be estimated as $\Gamma \sim \langle v_y^2 \rangle$ [46, 47]. Therefore, due to the energy balance $\dot{\gamma}\sigma \sim \Gamma$, the mean squared velocity is quadratic in the shear rate as $\langle v_y^2 \rangle \sim \eta\dot{\gamma}^2$, where the viscosity $\eta = \sigma/\dot{\gamma}$ is constant if the system is in the Newtonian regime. However, if the system is above jamming, the shear stress exhibits the yield stress σ_Y in the quasi-static limit, $\dot{\gamma} \rightarrow 0$. In this case, the energy balance equation tells us that the mean squared velocity is linear in the shear rate as $\langle v_y^2 \rangle \sim \dot{\gamma}\sigma_Y$.

Taking account of the dependence of $\langle v_y^2 \rangle$ on $\dot{\gamma}$, we describe the data in Fig. 1(a) as

$$\frac{\langle v_y^2 \rangle}{|\Delta\phi|^\psi} \sim \mathcal{F}\left(\frac{\dot{\gamma}}{|\Delta\phi|^\chi}\right) \quad (3)$$

with a scaling function $\mathcal{F}(x)$. In the Newtonian regime, the scaling function is quadratic, $\mathcal{F}(x) = x^2$ (dotted line in Fig. 1(a)), so that $\langle v_y^2 \rangle \sim |\Delta\phi|^{\psi-2\chi}\dot{\gamma}^2 = |\Delta\phi|^{-2.5}\dot{\gamma}^2$, indicating the viscosity divergence near jamming as $\eta \sim |\Delta\phi|^{-2.5}$ [6, 8, 9]. If the system is in the quasi-static regime above jamming, the scaling function is linear, $\mathcal{F}(x) = x$ (dashed line), such that $\langle v_y^2 \rangle \sim |\Delta\phi|^{\psi-\chi}\dot{\gamma} = |\Delta\phi|^{1.0}\dot{\gamma}$. This means that the yield stress scales as $\sigma_Y \sim |\Delta\phi|^{1.0}$ [6]. In the $\Delta\phi$ -independent critical regime, the scaling function is $\mathcal{F}(x) = x^z$ with the exponent z . From Eq. (3), we find $\langle v_y^2 \rangle \sim |\Delta\phi|^{\psi-\chi z}\dot{\gamma}^z$ which should not depend on $\Delta\phi$. Therefore, the exponents satisfy $\psi - \chi z = 0$, i.e. $z = \psi/\chi$, as indicated by the solid line in Fig. 1(a).

Critical scaling of relaxation time.— Next, we analyze the velocity auto-correlation function $C(\tau)$ in the GK formula (Eq. (2)). Figure 2(a) displays our numerical results of $C(\tau)$ (symbols), where $\dot{\gamma}t_0 = 10^{-6}$ is used in MD simulations and ϕ varies as listed in the legend. To describe our numerical results, we introduce a stretched exponential function as $C(\tau) = \exp[-(\tau/\tau_*)^\alpha]$, where α and τ_* are the stretching exponent and relaxation time, respectively [24, 25]. Adjusting the two parameters, α and τ_* , we can see good agreements between the data below jamming, $\phi < \phi_J$, and stretched exponential functions

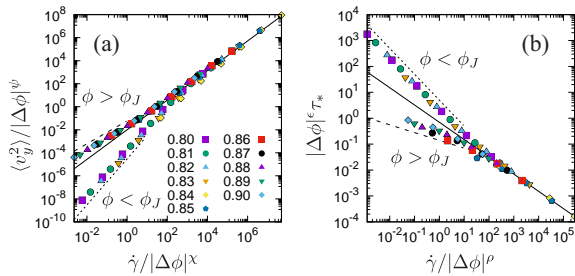


FIG. 1. Scaling collapses of (a) the mean squared transverse velocity $\langle v_y^2 \rangle$ and (b) relaxation time τ_* , where the scaling exponents are given by $\psi = 4.5$, $\chi = 3.5$, $\epsilon = 2.0$, and $\rho = 3.0$ (as listed in Table I). The solid lines have the slopes, (a) ψ/χ and (b) $-\epsilon/\rho$, and the symbols represent the packing fraction ϕ as listed in the legend of (a).

(solid lines). Note that α converges to unity if $\phi < \phi_J$ and $\dot{\gamma} \rightarrow 0$ (see SM [45]) so that $C(\tau)$ exponentially decays to zero in the Newtonian regime. We also find that the data above jamming, $\phi > \phi_J$, are well fitted to the stretched exponential functions if the shear rate is large enough, i.e. $\dot{\gamma}t_0 \geq 10^{-5}$. However, as we will discuss in later, $C(\tau)$ cannot be described as the stretched exponential function in a quasi-static regime above jamming, i.e. $\phi > \phi_J$ and $\dot{\gamma}t_0 \leq 10^{-6}$.

The relaxation time τ_* extracted from $C(\tau)$ exhibits critical scaling near jamming. Figure 1(b) shows scaling collapses of τ_* , where the scaling exponents are given by $\epsilon = 2.0$ and $\rho = 3.0$. The solid line with the slope $-\epsilon/\rho$ represents the $\Delta\phi$ -independent critical regime. In this figure, τ_* cannot be defined for quasi-static flows above jamming ($\phi > \phi_J$ and $\dot{\gamma}t_0 \leq 10^{-6}$).

To describe the data in Fig. 1(b), we introduce a scaling function $\mathcal{G}(x)$ as

$$|\Delta\phi|^\epsilon \tau_* \sim \mathcal{G}\left(\frac{\dot{\gamma}}{|\Delta\phi|^\rho}\right). \quad (4)$$

Based on our numerical results, we empirically determine the scaling function as follows: In the Newtonian regime, the scaling function is $\mathcal{G}(x) = x^{-1}$ (dotted line in Fig. 1(b)) so that the relaxation time scales as $\tau_* \sim |\Delta\phi|^{\rho-\epsilon}\dot{\gamma}^{-1} = |\Delta\phi|^{1.0}\dot{\gamma}^{-1}$. On the other hand, if the system is above jamming and the shear rate is large enough ($\dot{\gamma}t_0 \geq 10^{-5}$), the scaling function is $\mathcal{G}(x) = x^{-0.3}$ (dashed line), where the relaxation time scales as $\tau_* \sim |\Delta\phi|^{0.3\rho-\epsilon}\dot{\gamma}^{-0.3}$. In the $\Delta\phi$ -independent critical regime, the scaling function is $\mathcal{G}(x) = x^w$ (solid line), where the exponents satisfy $\rho w + \epsilon = 0$, i.e. $w = -\epsilon/\rho$.

The reduced Green-Kubo formula and scaling relations.— As long as the system is *not* in the quasi-static regime above jamming ($\phi > \phi_J$ and $\dot{\gamma}t_0 \leq 10^{-6}$), we can validate the GK relation and show that it is independent of the system size. Because the velocity auto-correlation function is well described as the stretched exponential function, we substitute $C(\tau) = \exp[-(\tau/\tau_*)^\alpha]$ into the

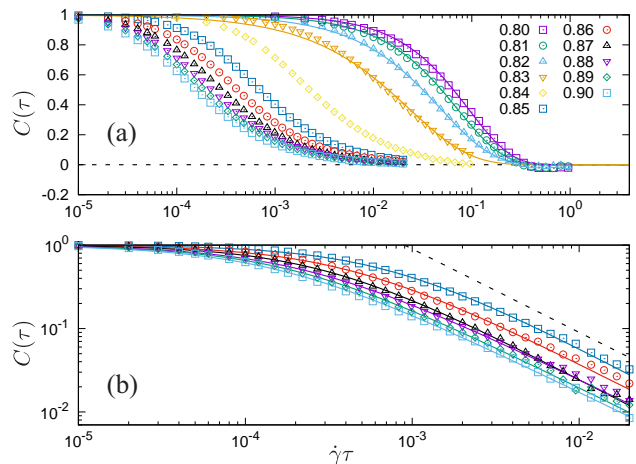


FIG. 2. (a) Semi-logarithmic and (b) double-logarithmic plots of the normalized velocity auto-correlation functions $C(\tau)$ (symbols), where $\dot{\gamma}t_0 = 10^{-6}$ and ϕ varies as listed in the legend of (a). The horizontal axes are scaled by $\dot{\gamma}$ and the solid lines are the fits to $C(\tau)$ (see the text for the details). The dashed line in (a) indicates zero and that in (b) shows the power-law decay, $C(\tau) \sim (\dot{\gamma}\tau)^{-1}$. In (b), only the data above jamming are shown.

GK formula. Calculating the time integral on the right-hand-side of Eq. (2), we find that the diffusion coefficient is given by

$$D = \frac{\tau_* \langle v_y^2 \rangle}{\alpha} \Gamma\left(\frac{1}{\alpha}\right). \quad (5)$$

As shown in Fig. 3(a), D extracted from the transverse MSD (Eq. (1)) and the right-hand-side of Eq. (5) coincide (solid line). In addition, Eq. (5) holds even if we change the number of particles N (Fig. 3(b)).

Substituting the critical scaling of D , $\langle v_y^2 \rangle$, and τ_* into the reduced GK formula (Eq. (5)), we clarify relationships between the critical exponents by analogy with *scaling relations* for critical phenomena. In the Newtonian regime, we found the critical scaling as $D \sim |\Delta\phi|^{-\nu}\dot{\gamma}$, $\langle v_y^2 \rangle \sim |\Delta\phi|^{\psi-2\chi}\dot{\gamma}^2$, and $\tau_* \sim |\Delta\phi|^{\rho-\epsilon}\dot{\gamma}^{-1}$. Neglecting the weak dependence of the stretching exponent α on the control parameters (ϕ and $\dot{\gamma}$), we substitute the critical scaling into $D \sim \tau_* \langle v_y^2 \rangle$ (Eq. (5)) and find $|\Delta\phi|^{-\nu}\dot{\gamma} \sim |\Delta\phi|^{\rho-\epsilon+\psi-2\chi}\dot{\gamma}$. Equating the exponents on both sides, we obtain the first scaling relation as

$$\nu + \psi - \epsilon = 2\chi - \rho. \quad (6)$$

TABLE I. Critical exponents.

D	$\langle v_y^2 \rangle$	τ_* ^a
$\nu = 1.0$	$\psi = 4.5$	$\epsilon = 2.0$
$\lambda = 4.0$	$\chi = 3.5$	$\rho = 3.0$

^a Except for the data in $\phi > \phi_J$ and $\dot{\gamma}t_0 \leq 10^{-6}$, where $C(\tau)$ exhibits the power-law decay (long-time tail).

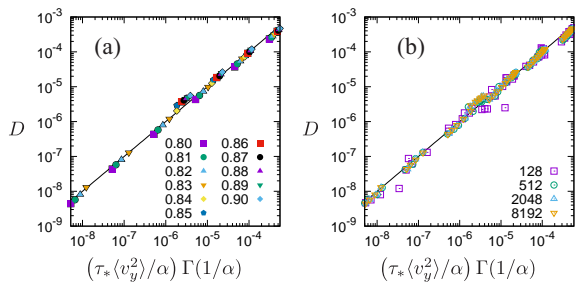


FIG. 3. (a) Parametric plots of the diffusion coefficient D extracted from the transverse MSD and the right-hand-side of Eq. (5), $(\tau_* \langle v_y^2 \rangle / \alpha) \Gamma(1/\alpha)$, where the system size is $N = 8192$ and the packing fraction ϕ increases as listed in the legend. (b) System size dependence of Eq. (5), where the number of particles N increases as listed in the legend. In both (a) and (b), the solid lines indicate $D = (\tau_* \langle v_y^2 \rangle / \alpha) \Gamma(1/\alpha)$.

If $\phi > \phi_J$ and $\dot{\gamma}t_0 \geq 10^{-5}$, the critical scaling is $D \sim |\Delta\phi|^{0.3\lambda - \nu} \dot{\gamma}^{0.7}$, $\langle v_y^2 \rangle \sim |\Delta\phi|^{\psi - \chi} \dot{\gamma}$, and $\tau_* \sim |\Delta\phi|^{0.3\rho - \epsilon} \dot{\gamma}^{-0.3}$. Substituting them into $D \sim \tau_* \langle v_y^2 \rangle$ (Eq. (5)), we find $|\Delta\phi|^{0.3\lambda - \nu} \dot{\gamma}^{0.7} \sim |\Delta\phi|^{0.3\rho - \epsilon + \psi - \chi} \dot{\gamma}^{0.7}$, where the exponents satisfy $\nu + \psi - \epsilon = \chi + 0.3(\lambda - \rho)$. By using Eq. (6), we obtain the second scaling relation as

$$\chi = 0.3\lambda + 0.7\rho. \quad (7)$$

In addition, $D \sim \dot{\gamma}^{1-\nu/\lambda}$, $\langle v_y^2 \rangle \sim \dot{\gamma}^{\psi/\chi}$, and $\tau_* \sim \dot{\gamma}^{-\epsilon/\rho}$ in the $\Delta\phi$ -independent critical regime. From Eq. (5), we find $\dot{\gamma}^{1-\nu/\lambda} \sim \dot{\gamma}^{\psi/\chi - \epsilon/\rho}$ such that the third scaling relation is given by

$$1 - \frac{\nu}{\lambda} = \frac{\psi}{\chi} - \frac{\epsilon}{\rho}. \quad (8)$$

Our numerical estimates of the critical exponents, ν , λ , ψ , χ , ϵ , and ρ (Table I), are roughly in accord with the scaling relations, Eqs. (6)-(8).

Long-time tails and finite-size effects on the diffusion coefficient.— If the system is in the quasi-static regime above jamming, i.e. $\phi > \phi_J$ and $\dot{\gamma}t_0 \leq 10^{-6}$, the data of $C(\tau)$ cannot be fitted to the stretched exponential functions. Figure 2(b) shows double-logarithmic plots of the data above jamming, $\phi > \phi_J$, where $C(\tau)$ exhibits the power-law decay in the long-time limit, i.e. *long-time tail* (dashed line). We find that the data are well described as $C(\tau) = \{1 + c(\dot{\gamma}\tau)^q\}^{-1}$ (solid lines), where $q \simeq 1$ and c weakly depends on ϕ (data are not shown) [48]. Note that the similar power-law decay of velocity auto-correlation function is also found at the onset of jamming transition, $\phi \simeq \phi_J$ [27], and MD simulations of granular particles sheared at constant pressure [48, 49].

If the long-time tail is observed as $C(\tau) \sim (\dot{\gamma}\tau)^{-1}$ (dashed line in Fig. 2(b)), the time integral in the GK formula (Eq. (2)) diverges. In recent numerical studies of sheared amorphous solids, it was reported that the diffusion coefficient over the shear rate scales as $D/\dot{\gamma} \sim L^\beta$

with the system length L and exponent $\beta \geq 1$ [33–39]. We also confirm that D linearly depends on L in the quasi-static regime above jamming, i.e. $\phi > \phi_J$ and $\dot{\gamma}t_0 \leq 10^{-6}$ (see SM [45]). Therefore, the diffusion coefficient diverges in the thermodynamic limit, $L \rightarrow \infty$, as expected by the long-time tail and the GK relation.

Discussion.— We have studied shear-induced diffusion of two-dimensional particles by MD simulations. Many previous works focused on the relation between diffusion coefficient D and length scales such as the cluster size ξ [28–31] and system length L [33–39]. In contrast, we have made a link between D and relaxation time τ_* through the reduced GK formula for non-equilibrium athermal systems, i.e. $D \sim \tau_* \langle v_y^2 \rangle$ (Eq. (5)). By using the energy balance equation, we have shown that the critical scaling of the mean squared transverse velocity $\langle v_y^2 \rangle$ well predicts the viscosity divergence, $\eta \sim |\Delta\phi|^{-2.5}$, and scaling of the yield stress near jamming, $\sigma_Y \sim |\Delta\phi|^{1.0}$ [6–11]. Except for quasi-static flows above jamming ($\phi > \phi_J$ and $\dot{\gamma}t_0 \leq 10^{-6}$), we have demonstrated scaling collapses of the relaxation time τ_* , where its non-trivial dependence on the control parameters, ϕ and $\dot{\gamma}$, was clarified. If the system is in the quasi-static regime above jamming, we found that the velocity auto-correlation function $C(\tau)$ exhibits the power-law decay, i.e. the long-time tail. In this case, the time integral in the non-equilibrium GK relation (Eq. (2)) diverges, implying finite-size effects on the diffusion coefficient [33–39]. Note that the shear-induced diffusion coefficient of three-dimensional particles does not diverge in the thermodynamic limit [36]. This means that the same scenario in classical fluids, where the GK relation is broken by long-time tails in two dimensions but is *not* in three dimensions [40], can be applied to our non-equilibrium athermal systems. In addition, we have proposed the scaling relations (Eqs. (6)-(8)) between the critical exponents (Table I) which are empirically estimated from numerical results. In future, we need to investigate the theoretical background to these exponents.

We thank B. P. Tighe, L. Berthier, H. Hayakawa, M. Otsuki, and S. Takada for fruitful discussions. This work was supported by KAKENHI Grant Nos. 20H01868, 21H01006, 22K03459, JPMJFR212T, 20H05157, 20H00128, 19K03767, 18H01188 from JSPS.

-
- [1] R. B. Bird, W. E. Stewart, and E. N. Lightfoot, *Transport Phenomena, Revised Second Edition* (John Wiley & Sons, Inc., 605 Third Avenue, New York, 2007).
 - [2] M. van Hecke, J. Phys.: Condens. Matter **22**, 033101 (2010).
 - [3] A. J. Liu and S. R. Nagel, Annu. Rev. Condens. Matter Phys. **1**, 347 (2010).
 - [4] C. S. O’Hern, L. E. Silbert, A. J. Liu, and S. R. Nagel, Phys. Rev. E **68**, 011306 (2003).
 - [5] H. Mizuno, K. Saitoh, and L. E. Silbert, Phys. Rev. E

- 93**, 062905 (2016).
- [6] P. Olsson and S. Teitel, Phys. Rev. Lett. **99**, 178001 (2007).
- [7] B. P. Tighe, E. Woldhuis, J. J. C. Remmers, W. van Saarloos, and M. van Hecke, Phys. Rev. Lett. **105**, 088303 (2010).
- [8] T. Kawasaki, D. Coslovich, A. Ikeda, and L. Berthier, Phys. Rev. E **91**, 012203 (2015).
- [9] P. Olsson, Phys. Rev. Lett. **122**, 108003 (2019).
- [10] B. P. Tighe, Phys. Rev. Lett. **107**, 158303 (2011).
- [11] K. Saitoh, T. Hatano, A. Ikeda, and B. P. Tighe, Phys. Rev. Lett. **124**, 118001 (2020).
- [12] F. m. c. Boyer, E. Guazzelli, and O. Pouliquen, Phys. Rev. Lett. **107**, 188301 (2011).
- [13] B. Andreotti, J.-L. Barrat, and C. Heussinger, Phys. Rev. Lett. **109**, 105901 (2012).
- [14] A. Ikeda, L. Berthier, and P. Sollich, Phys. Rev. Lett. **109**, 018301 (2012).
- [15] E. Lerner, G. Düring, and M. Wyart, Proc. Natl. Acad. Sci. U. S. A. **109**, 4798 (2012).
- [16] K. Suzuki and H. Hayakawa, Phys. Rev. Lett. **115**, 098001 (2015).
- [17] C. S. Campbell, J. Fluid Mech. **348**, 85 (1997).
- [18] J. Geng and R. P. Behringer, Phys. Rev. Lett. **93**, 238002 (2004).
- [19] B. Utter and R. P. Behringer, Phys. Rev. E **69**, 031308 (2004).
- [20] C. Eisenmann, C. Kim, J. Mattsson, and D. A. Weitz, Phys. Rev. Lett. **104**, 035502 (2010).
- [21] E. Wandersman, J. A. Dijksman, and M. van Hecke, Eur. Phys. Lett. **100**, 38006 (2012).
- [22] R. Cai, H. Xiao, J. Zheng, and Y. Zhao, Phys. Rev. E **99**, 032902 (2019).
- [23] R. Besseling, E. R. Weeks, A. B. Schofield, and W. C. K. Poon, Phys. Rev. Lett. **99**, 028301 (2007).
- [24] I. K. Ono, C. S. O'Hern, D. J. Durian, S. A. Langer, A. J. Liu, and S. R. Nagel, Phys. Rev. Lett. **89**, 095703 (2002).
- [25] I. K. Ono, S. Tewari, S. A. Langer, and A. J. Liu, Phys. Rev. E **67**, 061503 (2003).
- [26] T. Hatano, J. Phys. Conf. Series **319**, 012011 (2011).
- [27] P. Olsson, Phys. Rev. E **81**, 040301(R) (2010).
- [28] P. Kharel and P. Rognon, Phys. Rev. Lett. **119**, 178001 (2017).
- [29] P. Kharel and P. Rognon, Eur. Phys. Lett. **124**, 24002 (2018).
- [30] P. Rognon and M. Macaulay, Soft Matter **17**, 5271 (2021).
- [31] K. Saitoh and T. Kawasaki, Front. Phys. **8**, 99 (2020).
- [32] C. Heussinger, L. Berthier, and J.-L. Barrat, EPL **90**, 20005 (2010).
- [33] A. Lemaître and C. Caroli, Phys. Rev. E **76**, 036104 (2007).
- [34] A. Lemaître and C. Caroli, Phys. Rev. Lett. **103**, 065501 (2009).
- [35] J. Chattoraj, C. Caroli, and A. Lemaître, Phys. Rev. E **84**, 011501 (2011).
- [36] J. T. Clemmer, K. M. Salerno, and M. O. Robbins, Phys. Rev. E **103**, 042605 (2021).
- [37] B. Tyukodi, D. Vandembroucq, and C. E. Maloney, Phys. Rev. Lett. **121**, 145501 (2018).
- [38] B. Tyukodi, D. Vandembroucq, and C. E. Maloney, Phys. Rev. E **100**, 043003 (2019).
- [39] K. Martens, L. Bocquet, and J.-L. Barrat, Phys. Rev. Lett. **106**, 156001 (2011).
- [40] J. P. Hansen and I. R. MacDonald, *Theory of Simple Liquids* (Academic Press, Oxford, 1986).
- [41] T. Kawasaki and A. Onuki, Phys. Rev. E **87**, 012312 (2013).
- [42] T. Kawasaki and K. Kim, Sci. Adv. **3**, e1700399 (2017).
- [43] A. W. Lees and S. F. Edwards, J. Phys. C: Solid State Phys. **5**, 1921 (1972).
- [44] P. Olsson and S. Teitel, Phys. Rev. Lett. **109**, 108001 (2012).
- [45] See Supplemental Material at [URL will be inserted by publisher] for full details.
- [46] C. Heussinger, Phys. Rev. E **88**, 050201(R) (2013).
- [47] M. Maiti, A. Zippelius, and C. Heussinger, Eur. Phys. Lett. **115**, 54006 (2016).
- [48] E. DeGiuli, J. N. McElwaine, and M. Wyart, Phys. Rev. E **94**, 012904 (2016).
- [49] E. DeGiuli, G. Düring, E. Lerner, and M. Wyart, Phys. Rev. E **91**, 062206 (2015).